Contents list available at ScienceDirect

Radiation Measurements

journal homepage: www.elseviercom/locate/radmeas

In-field and out-of-file application in ^{12}C ion therapy using fully 3D silicon microdosimeters

Linh T. Tran[a], Lachlan Chartier[a,b], David Bolst[a], Jeremy Davis[a,f], Dale A. Prokopovich[a,b], Alex Pogossov[a], Susanna Guatelli[a,f], Mark I. Reinhard[a,b], Marco Petasecca[a,f], Michael L. F. Lerch[a,f], Naruhiro Matsufuji[c], Marco Povoli[d], Anand Summanwar[d], Angela Kok[d], Michael Jackson[e] and Anatoly B. Rosenfeld[a,f]

[a]Centre for Medical Radiation Physics, University of Wollongong, NSW, 2522, Australia
[b]Ionising Radiation, NSTLI Nuclear Stewardship, Australian Nuclear Science and Technology Organization, Lucas Heights, NSW 2234, Australia
[c]National Institutes for Quantum and Radiological Science and Technology, Chiba, Japan
[d]SINTEF, Norway
[e]University of New South Wales, Sydney NSW 2052, Australia
[f]Illawarra Health Medical Research Institute, Australia

HIGHLIGHTS

- The application of the silicon microdosimeters for radiation field characterisation in heavy ion therapy was presented
- Microdosimetric measurements were carried out and RBE_{10} values were derived in ^{12}C ion therapy
- Dose equivalent determination at different lateral points from the edge of the field were obtained

ARTICLE INFO

Article history:

Received Click here to enter the received date
Received in revised form Revised date
Accepted Accepted date
Available on line On-line date

Keywords:
Microdosimetry
Relative biological efficiency (RBE)
Charged particle therapy
Silicon microdosimeter
3D sensitive volume

ABSTRACT

This paper presents recent development of Silicon on Insulator (SOI) detectors for microdosimetry at the Centre for Medical Radiation Physics (CMRP) at the University of Wollongong. A new CMRP SOI microdosimeter design, the 3D mushroom microdosimeter is presented. Modification of SOI design and changes to the fabrication processes have led to improved definition of the microscopic sensitive volumes (SV), and thus to better modelling of the deposition of ionizing energy in a biological cell. The electrical and charge collection properties of the devices have been presented in previous works. In this study, the response of the microdosimeters in monoenergetic and spread out Bragg peak therapeutic ^{12}C ion beam at Heavy Ion Medical Accelerator in Chiba (HIMAC, Japan) are presented. Derived relative biological effectiveness (RBE) in ^{12}C ion radiation therapy matches the tissue equivalent proportional counter (TEPC) well, along with outstanding spatial resolution. The use of SOI technology in experimental microdosimetry offers simplicity (no gas system or HV supply), high spatial resolution, low cost, high count rates capabilities for beam characterization and quality assurance (QA) in charged particle therapy.

1350-4487 © Copyright Year,
doi: 10.1016/…

1. Introduction

Radiotherapy using heavy ion beams such as Carbon-ions is advantageous for the treatment of deep-seated tumors over conventional radiotherapy with X-rays due to an enhanced dose deposition in the Bragg peak (BP) at the end of the ion range. The high localization of dose delivery ensures the highest dose deposited in the tumour with minimal dose to the surrounding healthy tissue. Furthermore, the Relative Biological Effectiveness (RBE) of ^{12}C ions used in hadron therapy greatly depends on the depth of the target volume in the body due to LET variation, nuclear fragmentation processes and neutron productions. Due to the complexity of the field, it is important to estimate the RBE of the heavy ions in hadron therapy applications so as to deliver the correct dose.

Microdosimetry is an extremely useful technique for estimating the RBE in unknown mixed radiation fields, typical for hadron therapy. The conventional detector for microdosimetry is the tissue equivalent proportional counter (TEPC) which has the advantages of i) an isotropic response thanks to the spherical sensitive volume and ii) tissue equivalence of its walls and filling gas. However, the TEPC has several limitations such as high voltage operation, large size of assembly, which reduces spatial resolution and introduces wall effects, and an inability to simulate multiple cells.

The Centre for Medical Radiation Physics (CMRP) has developed multiple generations of microdosimeters on silicon-on-insulator (SOI) substrates which have been successfully tested [1-6] and recently summarized in [7]. The latest development of SOI microdosimeters at CMRP is the 3D array microdosimeter (also called “mushroom” microdosimeters) using 3D micro technology at SINTEF MiNaLab, Norway. The charge collection properties have been presented in [8].

This paper presents the response of the 3D mushroom microdosimeter in a therapeutic ^{12}C ion beam in HIMAC, Japan and shows its application for relative biological effectiveness (RBE) determination in charged particle therapy.

2. Material and Method

Design of the 3D mushroom microdosimeter

Figure 1 shows a schematic of two different single 3D SV structures of the mushroom microdosimeters. The first structure is called a trenched 3D (or air-trenched) SV and consists of 3D cylindrical SVs with a core column of air and n$^+$ doping in the inner walls of the SV center (Fig.1a). Each SV is surrounded with a trench of air and with p$^+$ doping on the outer wall, designed to physically eliminate the possibility of charge generated outside the SV from being collected.

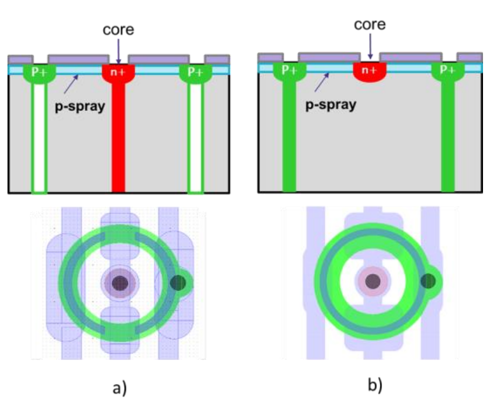

Figure 1 Schematics illustrating different configurations designed to define the sensitive volume geometry a) Trenched 3D structure (air-trenched) and b) Trenched planar structure (poly-trenched).

The second structure of the mushroom microdosimeter is called a trenched planar (or poly-trenched) SV, which also consists of 3D cylindrical SVs with a planar n$^+$ core produced by ion implantation (planar technology). Each SV is surrounded with a completely p$^+$ doped trench filled with polysilicon (Fig 1b).

The mushroom microdosimeter is based on an array of 2500 cylindrical SVs, each with a diameter of 30 µm and a thickness of 9.1 µm. The even and odd rows of SVs are read out independently to avoid events in adjacent sensitive volumes being read as a single event in the case of oblique charged particle tracks.

Microdosimetric probe based on SOI microdosimeter

Figure 2 shows the microdosimetric probe, named the Micro Plus probe (μ^+), developed at the CMRP, based on an SOI microdosimeter with an array of 3D SVs connected to a low noise spectroscopy-based readout circuit. The readout electronics of the μ^+ probe are located 10 cm away from the detector to keep the readout circuitry out of the primary radiation field and avoid radiation damage to the electronics. The $\mu+$ probe is covered by a PMMA sheath to allow the microdosimeter to be operated in water.

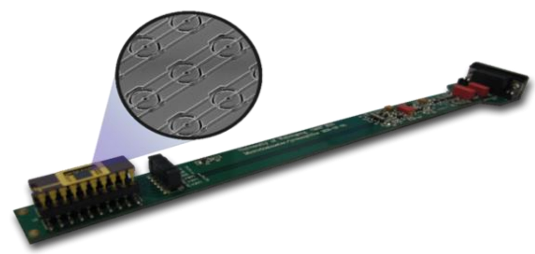

Figure 2 The microdosimetric probe (or also called MicroPlus probe)

Passive pristine Bragg Peak and Spread Out Bragg Peak (SOBP) of ^{12}C ion beam delivery at HIMAC facility.

A 290 MeV/u ^{12}C ion beam was delivered with pristine BP and SOBP of 60 mm using an Al ridge filter. A 0.434 mm and 0.649 mm Ta scatterer was used upstream to broaden the beam for the pristine and SOBP beams, respectively. Once shaped the beam was collimated to 10×10 cm^2 140 mm before the phantom. The range of the 290 MeV/u ^{12}C beam in water after traveling through air between nozzle and phantom was 147.92 mm. The microdosimetric probe was mounted in a water phantom using an X-Y stage to remotely control the detector location in the phantom with sub-hundred micron precision.

Data collection and analysis

The spectral response of the detector was recorded with an Amptek MCA 8000A Multi Channel Analyzer (MCA). To obtain the microdosimetric quantities from the MCA spectrum, the energy deposited was converted to lineal energy which is used to describe the energy deposition in a micron sized sensitive volume (SV) along a particle’s track, given by:

$$y = \frac{\varepsilon}{< l >} \tag{1}$$

where ε is the energy deposited in a SV with an average chord length $<l>$. A silicon-tissue scaling factor of 0.58 was obtained by calculating the energy deposition in silicon SV exposed to the 290 MeV/u ^{12}C ion radiation field, along the Bragg curve, by means of Geant4 [9].

Based on equation (1), the probability density $f(y)$ can be measured for all primary and secondary particles generated during an exposure to tissue by ionizing radiation. The dose probability density $d(y)$ is given by:

$$d(y) = \frac{y f(y)}{y_F} \tag{2}$$

where $\overline{y_F} = \int_0^\infty yf(y)dy$, $\overline{y_F}$ is the frequency-mean lineal energy. The dose-mean lineal energy $\overline{y_D}$ is defined as $\overline{y_D} = \int_0^\infty yd(y)dy$; the latter is used to determine the α parameter in the Linear Quadratic Model (LQM) applied for radiation field of interest and used later as an input parameter for the MKM to calculate RBE_{10} corresponding to 10% of human salivary gland (HSG) cell survival. A detailed description for calculating RBE_{10} using the MK model can be found in [10].

Determination of Quality factor and dose equivalent in out-of-field measurements

The dose-equivalent H is defined as the product of the absorbed dose and a quality factor used to estimate the dose received by a person upon radiation exposure. Using the lineal energy dependent quality factor Q(y), defined for radiation protection in the ICRU-40 report [11], the dose is scaled to be proportional to the biological effects it causes with respect to effects produced by a reference radiation. The method for calculating the dose-equivalent using microdosimetry has been explained in detail in previous work [12].

3. Results

Response of the microdosimeter to 290 MeV/u ^{12}C pristine BP

Figure 3 shows the dose-mean lineal energy values obtained at different depths in water obtained with the poly-trenched mushroom microdosimeter as well as the physical dose measured using a pin point ionisation chamber PTW31006 (0.015 cm^3 measuring volume) for the passively delivered 290 MeV/u pristine ^{12}C ion beam. The $\overline{y_D}$ values at the entrance depth in water was 11.39 keV/µm then increased up to approximately 90 keV/µm at the BP (147.92 mm depth in water) and then sharply rose up to 265 keV/µm at the distal part of the BP. This sharp increase in $\overline{y_D}$ can only be obtained due to the extremely high spatial resolution of the SOI microdosimeter of an order of 10 µm thick.

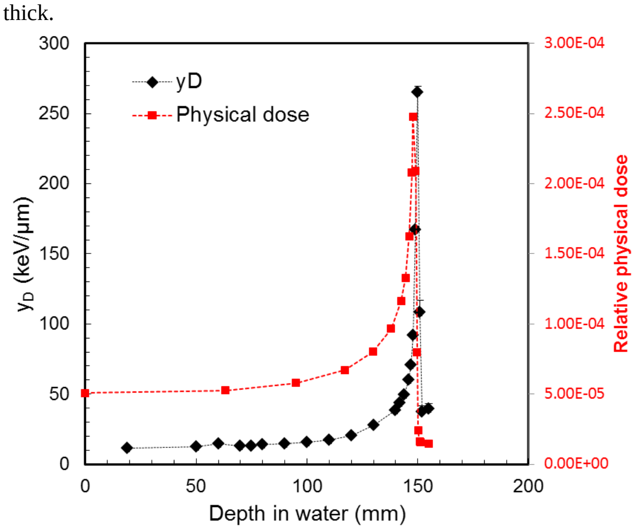

Figure 3 Dose mean lineal energy obtained with poly-trenched mushroom microdosimeter and corresponding physical dose in response to 290 MeV/u pristine ^{12}C ions.

Figure 4 shows the derived RBE_{10} distribution obtained with the poly-trenched mushroom microdosimeter at different depths in water and the corresponding physical dose, irradiated by a 290 MeV/u pristine BP of ^{12}C ion beam. Fig. 4 shows that for pristine ^{12}C ions the maximum RBE_{10} value of 2.92 occurs at the same depth as the physical dose, unlike other ions [13]. At the distal part of the BP the maximum $\overline{y_D}$ was approximately 265keV/µm, RBE_{10} was about 2.66. The decrease of RBE_{10} towards the distal part of the BP is associated with the overkilling effect of cells which has been taken into account by the MK model [7].

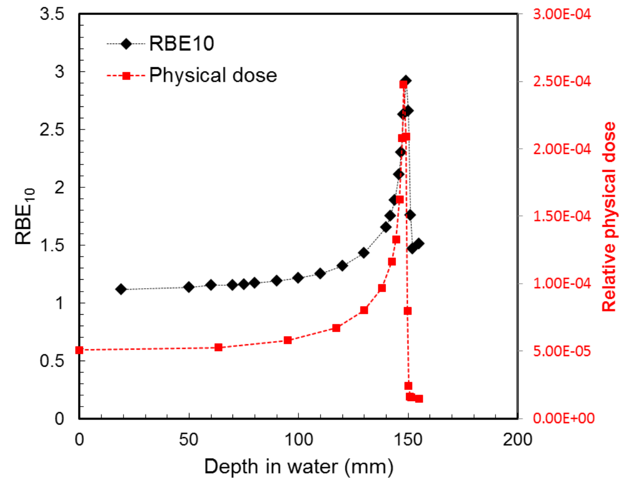

Figure 4 RBE_{10} obtained from measurements with the poly-trenched mushroom microdosimeter in 290 MeV/u pristine BP of ^{12}C ion beam.

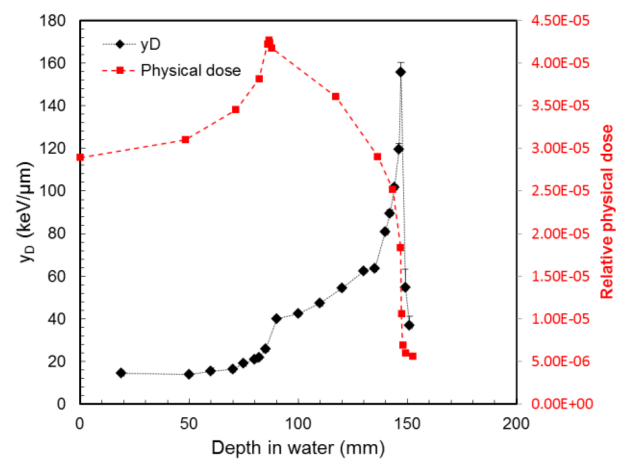

Figure 5 Dose mean lineal energy obtained with the poly-trenched mushroom microdosimeter and corresponding physical dose in response to 290 MeV/u ^{12}C SOBP.

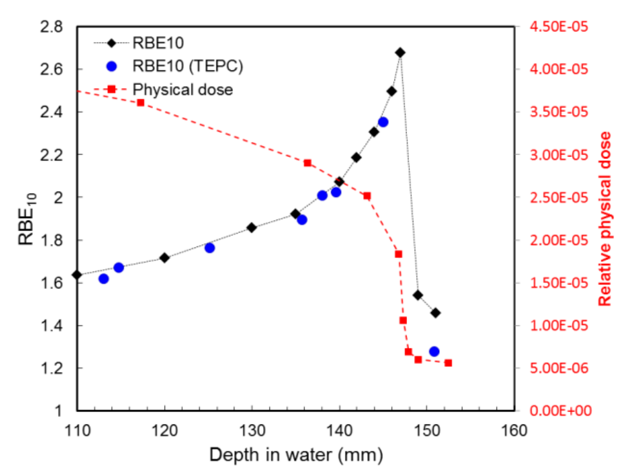

Figure 6 RBE_{10} obtained from the measurements with the poly-trenched mushroom microdosimeter and TEPC and corresponding physical dose in 290 MeV/u ^{12}C SOBP ions in water.

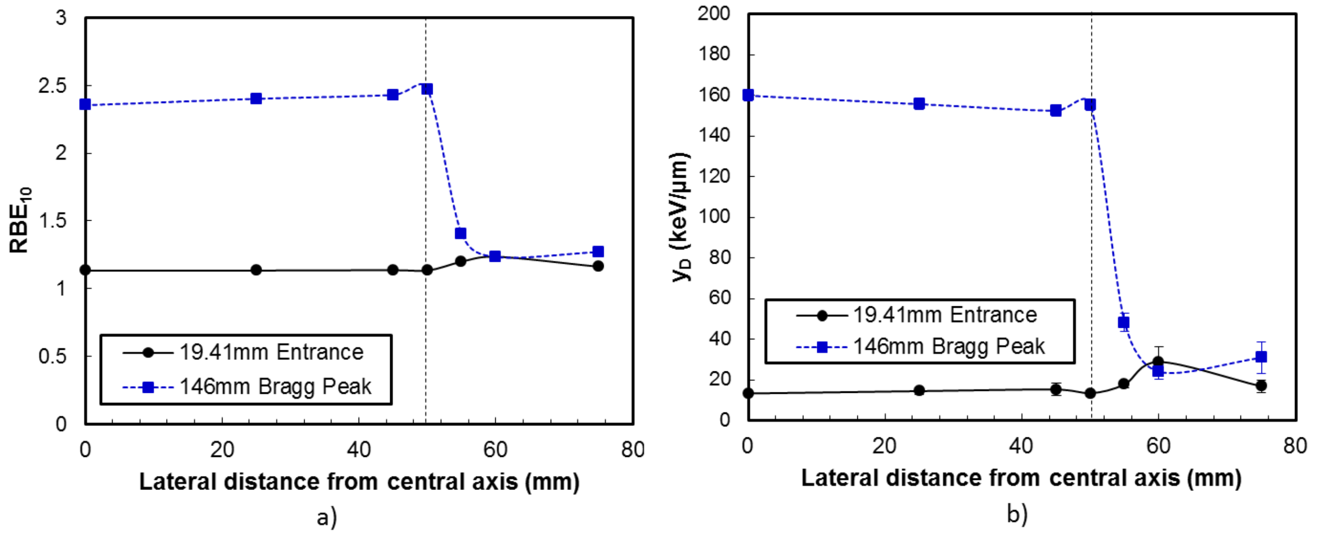

Figure 7 RBE10 (a) and $\overline{y_D}$ (b) lateral distributions at 19.41 mm and 146 mm depth of 290 MeV/u ^{12}C SOBP in water where the field size was 10 cm × 10 cm. The vertical dashed line shown in the graphs indicates the edge of the radiation field.

Figure 5 and 6 show the $\overline{y_D}$ and derived RBE$_{10}$ distributions in different depths in water obtained by the poly-trenched mushroom microdosimeter for a 290 MeV/u 60 mm ^{12}C SOBP, respectively. The physical dose measured by the pinpoint ionisation chamber is also shown. In order to deliver a flat biological dose in the target region, the ridge filter delivers a physical dose which decreases with depth such that $D_{biological} = D_{physical} \times RBE_{10}$ is flat over the 60 mm treatment area. The maximum $\overline{y_D}$ value obtained in the SOBP ^{12}C ion beam was 155.7 keV/µm and is lower than the maximum $\overline{y_D}$ value in the ^{12}C pristine BP. This is due to the presence of the Al ridge filter which smears out the sharp dose at the BP region due to increased straggling.

Figure 7 shows the RBE$_{10}$ and $\overline{y_D}$ lateral distributions at 19.41 mm and 146 mm depth in water where the field size was 10 cm × 10 cm. The air-trenched mushroom microdosimeter was used for this measurement and was placed at: 0, 25, 45, 50, 55, 60 and 70 mm from the central axis of the beam where 50 mm lateral distance is the edge of the radiation field. At the entrance of the SOBP (19.41 mm depth), it can be seen that the RBE$_{10}$ values were almost constant in the field however at the penumbra region the RBE$_{10}$ slightly increased from 1.13 to 1.23 as the microdosimeter moved 5 to 10 mm out of the field due to fragments and neutrons. Finally the RBE$_{10}$ slightly decreased as the microdosimeter was moved further away.

At the end of the SOBP region (146 mm depth), the RBE$_{10}$ values were also almost constant in the field and then dropped sharply at the penumbra region. At 5 mm distance from the edge of the field, the RBE$_{10}$ reduced from 2.47 down to 1.44 and stayed almost constant at further lateral distances due to the contribution of fragments with lower LET than that of the primary ^{12}C ions at the end of their range, but higher than recoiled protons, generated from neutrons. At larger distances, the effects of neutrons and fragmented protons are not distinguishable. A similar trend was observed with the $\overline{y_D}$ distribution shown in Figure 7b. For 19.41 mm depth both $\overline{y_D}$ and RBE$_{10}$ are constant within the field while towards the edge of the field $\overline{y_D}$ slightly decreases at 146 mm depth leading to a slight increase in RBE$_{10}$ due to the correction for the overkilling effect by the MK model.
The RBE$_{10}$ and $\overline{y_D}$ values provide useful information on how the RBE$_{10}$ and $\overline{y_D}$ varies at the penumbra region, particularly for the sharp dose gradients at the edge of the field.

Determination of dose equivalent in penumbra region of the 290 MeV/u ^{12}C beam

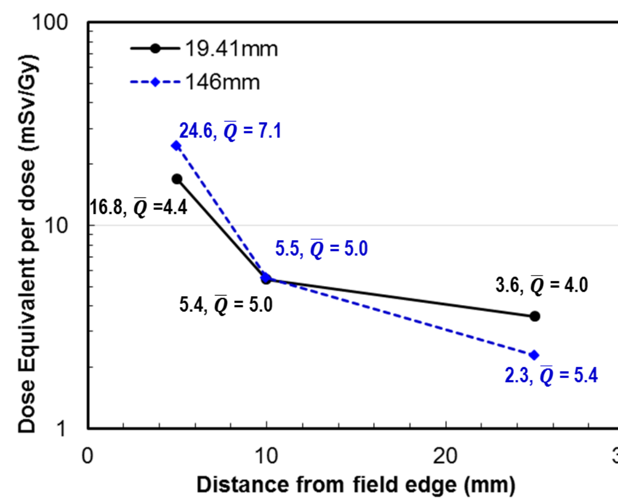

Figure 8 Dose equivalent per dose and calculated average quality factor at different lateral points from the edge of field for 19.41 mm and 146mm depth in water.

Figure 8 shows the dose equivalent per dose in the middle of the SOBP which was calculated based on the measured lineal energy spectra obtained with the air-trenched mushroom microdosimeter at lateral distances of 5 mm, 10 mm and 25 mm from the edge of the carbon SOBP field for depths 19.41 mm and 146 mm. At a 5 mm lateral distance from the field edge the dose equivalent was 24.6 mSv/Gy and 16.8 mSv/Gy for 146 mm and 19.41 mm depth, respectively. The dose equivalent at these points correlate with an average quality factor Q ($\bar{Q}$) of 7.1 and 4.4 for 146 mm and 19.41 mm depth, respectively. Increasing $\bar{Q}$ can be explained by the contribution of primary ^{12}C scattered ions which have lower energy at 146 mm depth in comparison to 19.41 mm depth. At 10 mm lateral distance from the field edge the dose equivalent and $\bar{Q}$ obtained at 2 depths were approximately the same. At 25 mm lateral distance the dose equivalent dropped faster laterally at 146 mm depth in comparison with 19.41 mm depth while $\bar{Q}$ is in opposite correlation with values of 5.4 and 4.0, respectively. This can be explained due to larger partial contribution of heavier fragments and fast neutrons at 146 mm depth in comparison to the shallower depth 19.41 mm, while physical dose due to fragments is lower at depth 146 mm than at 19.41 mm depth for this lateral point.

4. Conclusion

Two SOI mushroom microdosimeters structures have been recently developed, fabricated and characterised in pristine and SOBP ^{12}C ion beams at HIMAC, Japan. The dose mean lineal energy and RBE_{10} distributions in water were obtained with exceptionally high spatial resolution in the BP and the distal part of the BP. This work has shown that the $\overline{y_D}$ at the entrance of the ^{12}C pristine BP (11.3 keV/µm) was lower than that obtained at the entrance of the SOBP (14.5 keV/µm). However the maximum $\overline{y_D}$ values in the pristine BP was higher than those in the SOBP due to the presence of an Al ridge filter. The maximum RBE_{10} values for ^{12}C ions occurred at the same depth as the maximum physical dose in the BP which is in agreement with other work [13]. This confirms the advantage of using ^{12}C ion for treatment of tumours.

The results obtained by the SOI microdosimeters show good agreement with the TEPC after the application of proper correction factors to convert the silicon response to that biological tissue and indicate that the mushroom microdosimeter is suitable for use in heavy ion therapy applications.

The lateral RBE_{10} and dose mean lineal energy distributions were obtained in this study for a depth close to the entrance and a depth at the end of the SOBP. It has been shown that in the penumbra region the lateral RBE_{10} sharply decreased for 146 mm depth and slightly increased for 19.41 mm depth. The dose equivalent at these lateral points were also estimated. The dose equivalent reduced over a short distance for lateral points at 19.41 mm depth in comparison with 146 mm depth.

The silicon microdosimeter containing 3D SVs presented in this study is a new and fast radiation field characterisation tool that has been tested and applied in heavy ion therapy applications with sub-millimetre spatial resolution. It shows great promise as an experimental device used for microdosimetric spectra measurements and based on this, commissioning of RBE used in treatment planning systems.

Acknowledgement

This research was supported by the Australian Government through the Australian Research Council's Discovery Projects funding scheme (project DP 170102273).

The authors would like to acknowledge Dr. Nadia Court and her team at the UNSW ANFF node for their packaging work as well as Mr. Adam Sarbutt from NSTLI Nuclear Stewardship, ANSTO and Mr. Peter Ihnat from the School of Physics, UOW for their assistance in preparation for the experiment. Finally the authors would like to thank all collaborators in the 3D-MiMiC project, funded by the Norwegian Research Council via the NANO2021 program.

References

[1] P. D. Bradley, "The development of a novel silicon microdosimeter for High LET radiation therapy," Ph.D. dissertation, Fac. Eng., Univ. Wollongong, Wollongong, Australia, 2000.

[2] A. L. Ziebell, W. H. Lim, M. I. Reinhard, I. Cornelius, D. A. Prokopovich, R. Siegele, A. S. Dzurak, and A. B. Rosenfeld, "A cylindrical silicon-on-insulator microdosimeter: charge collection characteristics," IEEE Trans. Nucl. Sci., vol. 55, no. 6, pp. 3414-3420, Dec. 2008.

[3] D. A. Prokopovich, M. I. Reinhard, G. C. Taylor, A. Hands, A. B. Rosenfeld, "Comparison of SOI microdosimeter and tissue equivalent proportional counter measurements at the CERF facility," IEEE Trans. Nucl. Sci., vol. 59, no. 5, pp. 2501-2505, 2012.

[4] J. Livingstone, D. A. Prokopovich, M. L. F. Lerch, M. Petasecca, M. I. Reinhard, H. Yasuda, M. Zaider, J. Ziegler, V. L. Pisacane, J. Dicello, V. Perevetaylo, and A. B. Rosenfeld, "Large area silicon microdosimeter for dosimetry in high LET space radiation fields: charge collection study," IEEE Trans. Nucl. Sci., vol. 59, no. 6, pp. 3126-3132, Dec. 2012.

[5] L. T. Tran, Lachlan Chartier, Dale A. Prokopovich, Marco Petasecca, Michael L. F. Lerch, Mark I. Reinhard, Vladimir Perevetaylor, Naruhiro Matsufuji and Anatoly B. Rosenfeld, "3D-mesa "Bridge" silicon microdosimeter: charge collection study and application to RBE studies in 12C radiation therapy," IEEE Trans. Nucl. Sci., vol. 62, no. 2, pp. 504-511, Apr. 2015.

[6] L. T. Tran, Lachlan Chartier, David Bolst, Susanna Guatelli, Mark I. Reinhard, Marco Petasecca, Michael L. F. Lerch, Vladimir L. Pereverlaylo, Naruhiro Matsufuji, David Hinde, Mahananda Dasgupta, Andrew Stuchbery and Anatoly B. Rosenfeld, "3D Silicon Microdosimetry and RBE study using ^{12}C ion of different energies," IEEE Trans Nucl. Sci., vol. 62, no. 6, pp. 3027 – 3033, 2015.

[7] A. B. Rosenfeld, "Novel detectors for silicon based microdosimetry, their concepts and applications," Nucl. Instrum. Meth., Phys. Res. A, vol. 809, pp. 156–170, February 2016.

[8] Linh T. Tran, Lachlan Chartier, Dale A. Prokopovich, David Bolst, Marco Povoli, Anand Summanwar, Angela Kok, Alex Pogossov, Marco Petasecca, Susanna Guatelli, Mark I. Reinhard, Michael Lerch, Mitchell Nancarrow, Naruhiro Matsufuji, Michael Jackson and Anatoly B. Rosenfeld, "Thin Silicon Microdosimeter utilizing 3D MEMS Fabrication Technology: Charge Collection Study and its application in mixed radiation fields," IEEE Trans Nucl. Sci., 2017, DOI: 10.1109/TNS.2017.2768062.

[9] D. Bolst, S. Guatelli, L. T. Tran, L. Chartier, M. Lerch, N. Matsufuji and A. Rosenfeld, "Correction factors to convert microdosimetry measurements in silicon to tissue in ^{12}C ion therapy," Phys. Med. Biol., vol. 62, no. 6, pp. 2055-2069, 2017.

[10] Kase Y, Kanai T, Matsumoto Y et al. "Microdosimetric measurements and estimation of human cell survival for heavy-ion beams". Radiation Res. 2006; 166:629–38.

[11] International Commission on Radiation Units and Measurements, "The quality factor in radiation protection," Report ICRU-40, 1986.

[12] Linh T. Tran, Lachlan Chartier, David Bolst, Alex Pogossov, Susanna Guatelli, Dale A. Prokopovich, Marco Petasecca, Michael L. F. Lerch, Mark I. Reinhard, Benjamin Clasie, Nicolas Depauw, Hanne Kooy, Jay Flanz, Aimee McNamara, Harald Paganetti, Chris Beltran, Keith Furutani, Vladimir L. Perevertaylo, Michael Jackson and Anatoly B. Rosenfeld. "Characterisation of proton pencil-beam scanning using a high spatial resolution solid state microdosimeter", Medical Physics, doi: 10.1002/mp.12563, 2017.

[13] G. Kraft "Tumor Therapy with Heavy Charged Particles", Progress in Particle and Nuclear Physics 45(2000), 473-544